Supplementary Figures

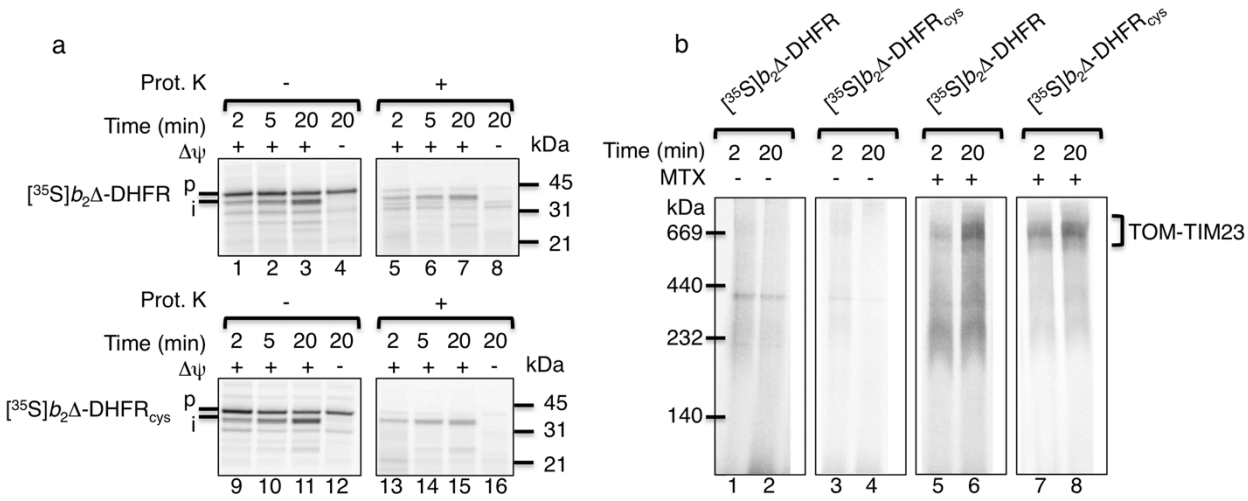

Supplementary Figure 1 - Properties of the cysteine-modified unlabelled preprotein substrate

(a) The radiolabelled preproteins b_2Δ-DHFR and b_2Δ-DHFR$_{cys}$ were imported into isolated mitochondria. Where indicated, the membrane potential (Δψ) was uncoupled by the addition of AVO mix (8 μM antimycin A, 1 μM valinomycin, 20 μM oligomycin) prior to the import reaction. Non-imported proteins were digested with 50 μg/ml proteinase K as indicated. Mitochondria were re-isolated by centrifugation, proteins were solubilized in Laemmli buffer and separated by SDS-PAGE. In the presence of Δψ, the preproteins are imported to a protease-protected location within mitochondria and the N-terminal presequence is proteolytically removed by the matrix-localized mitochondrial processing peptidase (MPP)[1]. The preprotein b_2Δ-DHFR and the derived preprotein b_2Δ-DHFR$_{cys}$ were imported with similar kinetics; p = preprotein, i = intermediate. (b) The different preproteins were imported into mitochondria as described in (a). Where indicated, 5 μM MTX was added to stabilize the folded state of the DHFR moiety, which causes preprotein arrest at mitochondrial import sites. This stalling event generates a two-membrane-spanning translocation intermediate, in which the TOM and TIM23 complexes are tethered

by the preprotein[2,3,4]. After mitochondrial re-isolation, protein complexes were solubilized in digitonin-containing buffer and separated by blue native electrophoresis. Stable folding of the DHFR domain caused the arrest of both the $b_2\Delta$-DHFR and the derived $b_2\Delta$-DHFR$_{cys}$ preprotein with comparable efficiency. The contrast of the gel lanes showing import of [^{35}S]$b_2\Delta$-DHFR (lanes 1, 2, 5, and 6) was linearly adjusted by digital processing to improve the visibility of the protein bands.

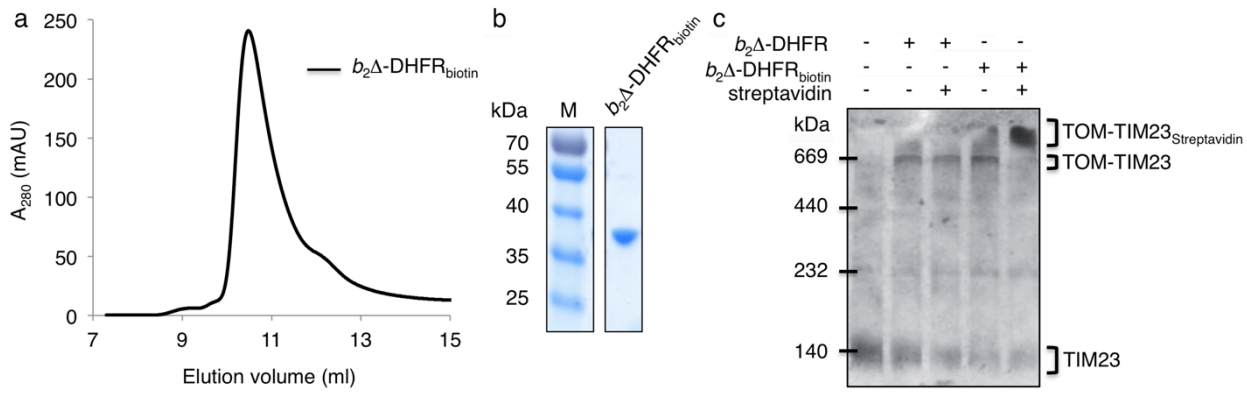

Supplementary Figure 2 – Purification of $b_2\Delta$-DHFR$_{biotin}$ and streptavidin shift assay

(a) $b_2\Delta$-DHFR$_{biotin}$ was purified by size-exclusion chromatography on a Supadex75 (10/300) column. (b) The resulting protein is resolved at 37 kDa via SDS-PAGE and Coomassie blue staining. M, molecular weight marker. Three different protein preparations were used in this work to confirm the reproducibility of results. (c) $b_2\Delta$-DHFR or $b_2\Delta$-DHFR$_{biotin}$ were accumulated in mitochondrial import sites in the presence of MTX. Preprotein-loaded mitochondria were subsequently incubated in the presence or absence of streptavidin as indicated. Samples were subjected to blue native electrophoresis and TOM-TIM23 supercomplexes were detected by western blotting with Tim23-specific antibodies. Streptavidin binding quantitatively shifts TOM-TIM23 supercomplexes containing stalled $b_2\Delta$-DHFR$_{biotin}$. The experiment was repeated three times.

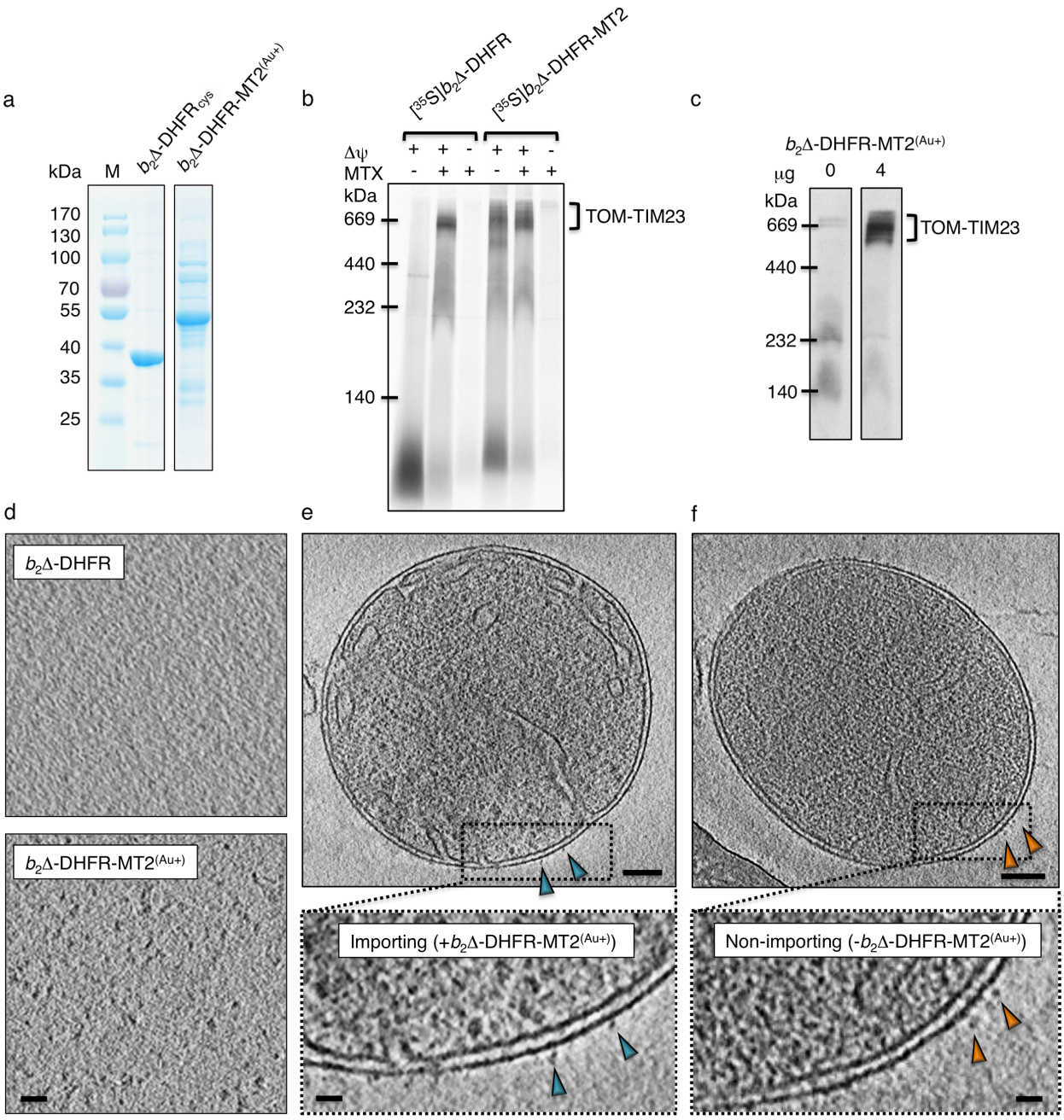

Supplementary Figure 3 – Characterization of b_2Δ-DHFR-MT2 as a tag for mitochondrial preprotein import

(a) After purification from *E. coli,* b_2Δ-DHFR$_{cys}$ and b_2Δ-DHFR-MT2$^{(Au+)}$ were resolved via SDS-PAGE and Coomassie blue staining at 37 kDa and 50 kDa respectively. M, molecular weight marker. (b) The radiolabelled preproteins b_2Δ-DHFR and b_2Δ-DHFR-MT2 were imported into isolated mitochondria. Where indicated, 5 μM MTX was added to stabilize

the folded state of the DHFR moiety, and the membrane potential ($\Delta\psi$) was uncoupled by the addition of AVO mix as described in Supplementary Fig. 1. Protein complexes were solubilized in digitonin-containing buffer for blue native electrophoresis. Stable folding of the DHFR domain in the presence of MTX caused translocation arrest of both preproteins. A fraction of $b_2\Delta$-DHFR-MT2 was arrested even in the absence of MTX. (c) Blue native electrophoresis and western blot analysis of the $b_2\Delta$-DHFR-MT2$^{(Au+)}$ tethered TOM-TIM23 supercomplex, detected with an antibody against Tim23. (d) Slices through tomograms demonstrate that $b_2\Delta$-DHFR-MT2$^{(Au+)}$ can be discriminated in solution; scale bar = 10 nm. A slice through a tomogram of (e) a $b_2\Delta$-DHFR-MT2$^{(Au+)}$ importing and (f) a non-importing mitochondrion, demonstrates that the metallothionein tag cannot be distinguished from protein densities on the surface of mitochondria (blue and orange arrowheads). 30 mitochondria were investigated in total; scale bars = 100 nm, insets = 10 nm.

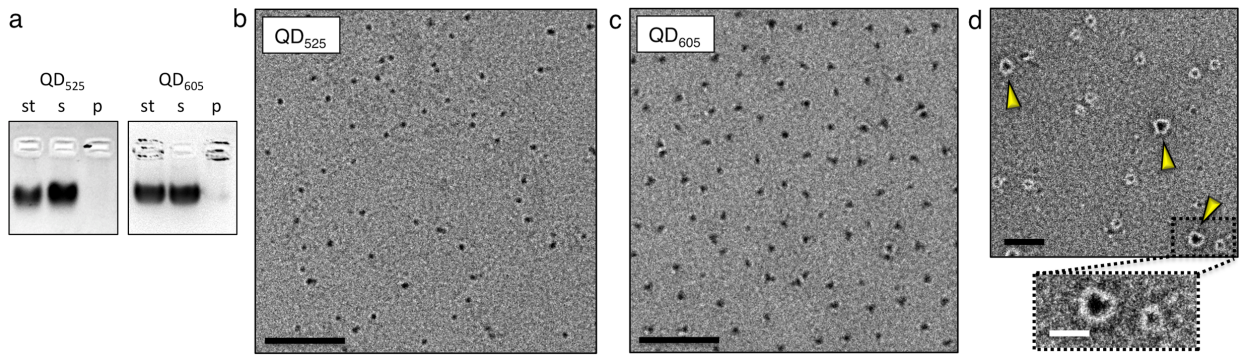

Supplementary Figure 4 –QD analysis

(a) QD_{525} and QD_{605} were separated by agarose gel electrophoresis; st = 1 μM starting material. QDs were centrifuged prior to labelling experiments; s = supernatant, p = pellet. Aggregated material was observed in the gel wells for the starting material and pellet for QD_{605}, but was negligible for QD_{525}. No higher order species were observed in either supernatant, which were subsequently used for labelling. The experiment was repeated 3 times. (b & c) Negative stain electron micrographs show the sizes of QD_{525} and QD_{605} dense cores. QD_{525} measures ~4 nm and QD_{605} ~4 nm x 9 nm; scale bars = 100 nm. (d) On more heavily stained grids containing both types of QDs, a white halo of surrounding low-density material (PEG linker plus streptavidin) was seen surrounding the dense core. QD_{605} is marked with yellow arrowheads and QD_{525} is unmarked. The total size of QD_{605} measures ~19 nm and QD_{525} ~12 nm; scale bar = 50 nm, inset = 20 nm.

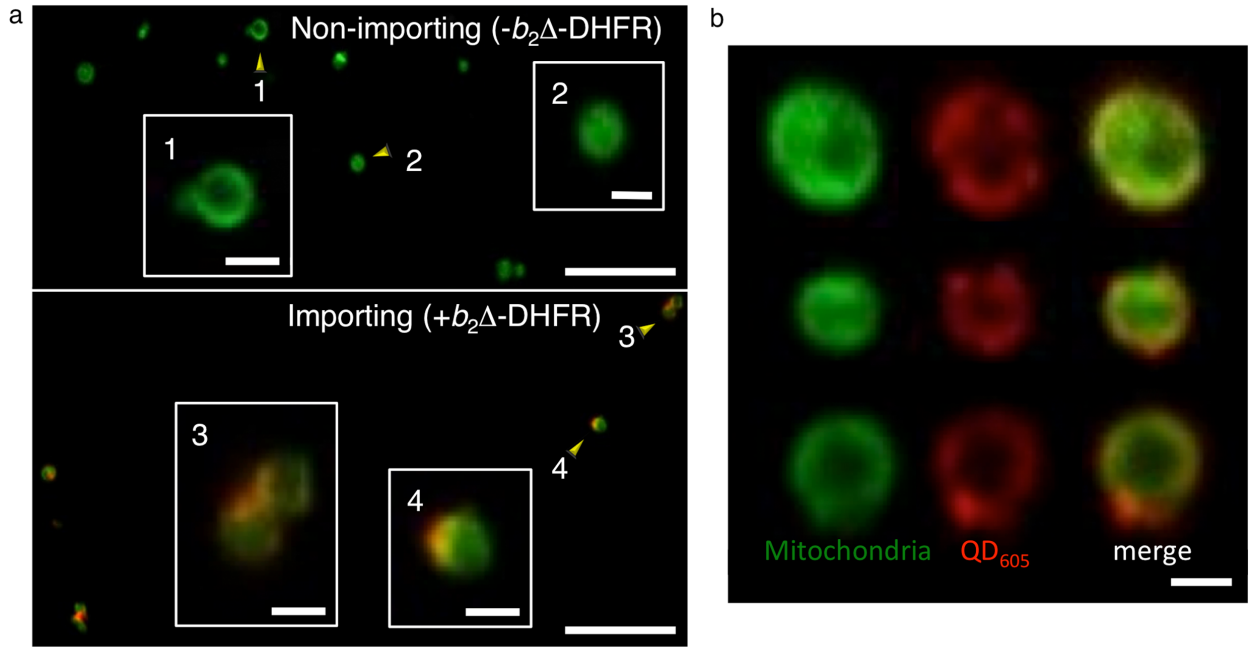

Supplementary Figure 5 – Analysis of importing mitochondria by confocal microscopy

(a) Confocal fluorescence images of non-importing and importing mitochondria, both incubated with QDs and separated via an Optiprep gradient. The mitochondria are labelled with MitoTracker Green and QD_{605} fluorescence is shown in red. Yellow arrowheads and the numbered insets show magnification views of 4 representative image areas; scale bars = 10 μm; insets = 1 μm. (b) Close-ups of three importing mitochondria show the distribution of QD_{605} around the mitochondrial surface. Left: green channel emission showing mitochondria labelled with MitoTracker Green; centre: red channel emission showing QD_{605} localization, right: overlay of both signals; scale bar = 1 μm.

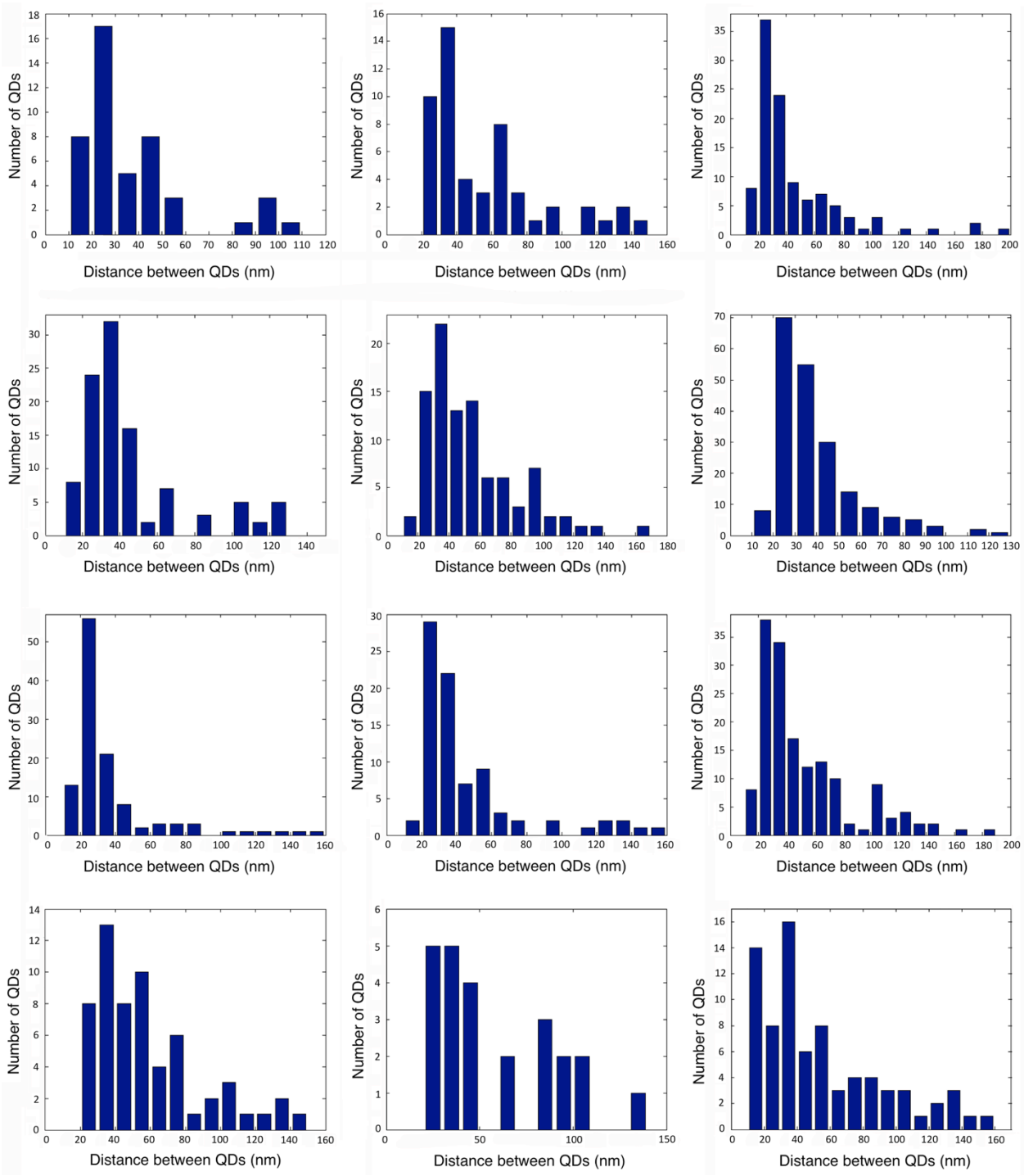

Supplementary Figure 6 – Calculation of the closest QD-QD distances

Histograms showing the closest distance between two QDs, calculated from 12 individual mitochondrial samples, accumulating 1159 QD_{605} data points in total.

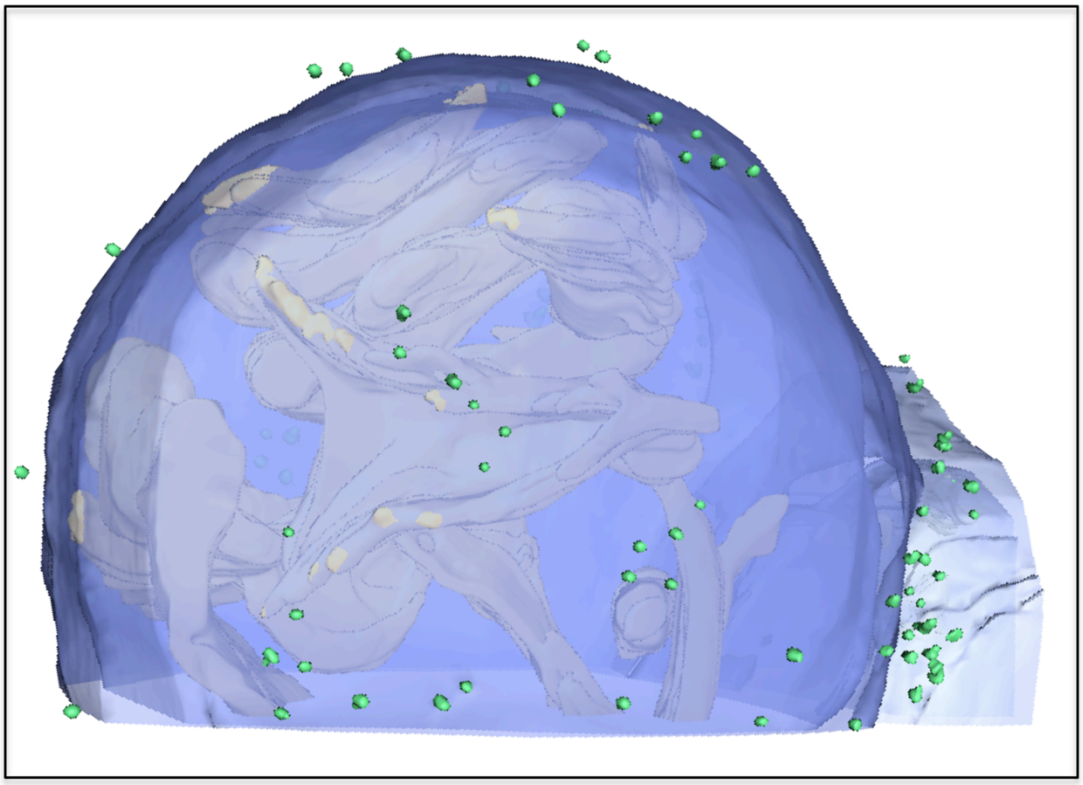

Supplementary Figure 7 – The sites of preprotein import may be visualized on all surfaces

Segmentation of the full tomographic volume reveals the location of QDs (green spheres) on both upper and lower surfaces, and in proximity to the mitochondrial fusion septum. The outer membrane is rendered in two colors (light and dark blue) in order to distinguish the position of the septal ring distinct from the cristae (yellow).

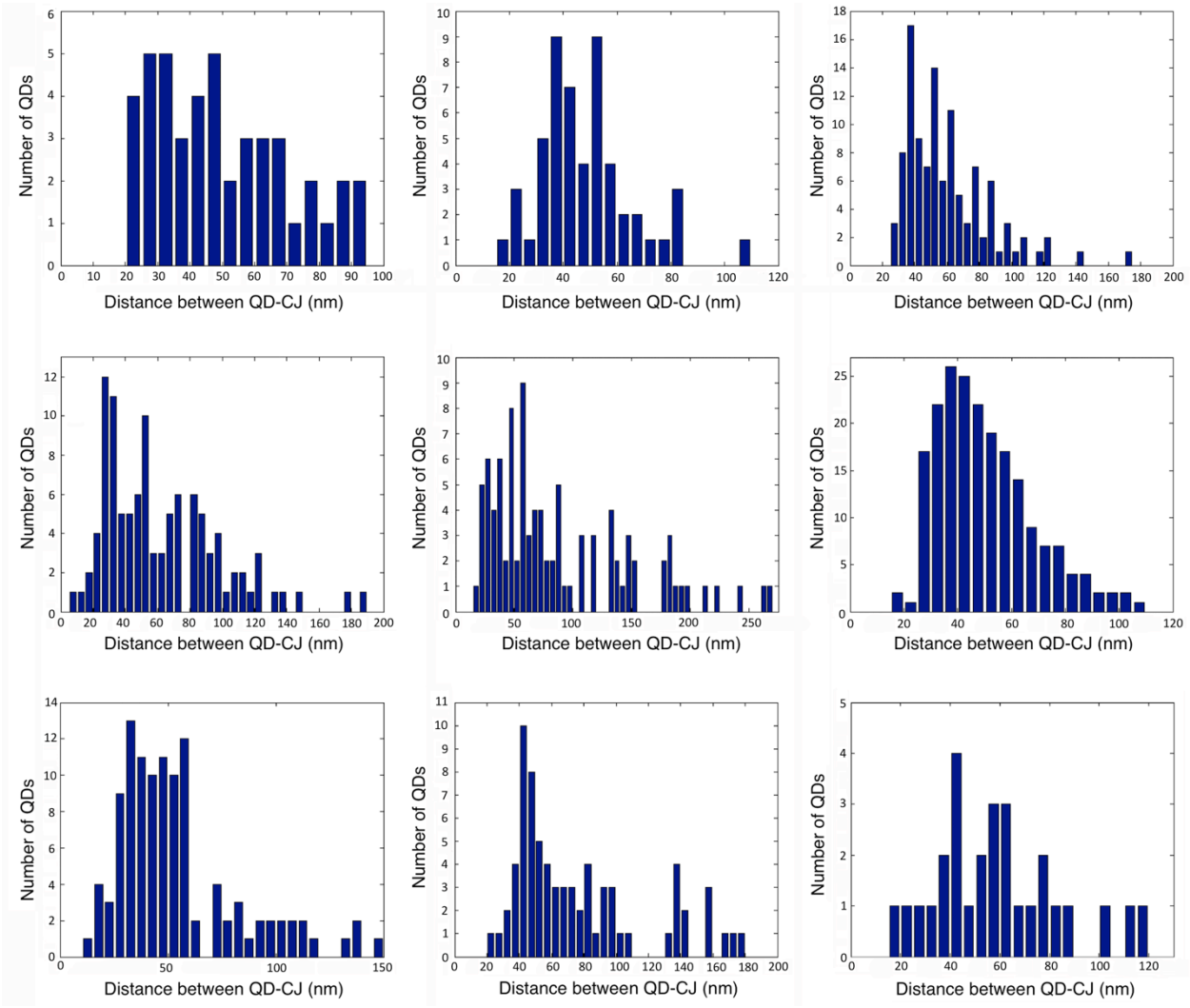

Supplementary Figure 8 – Calculation of the closest QD-crista junction distances

Histograms showing the closest distance between QD and crista junction (CJ), calculated from 9 individual mitochondrial samples, accumulating 836 QD_{605} data points in total.

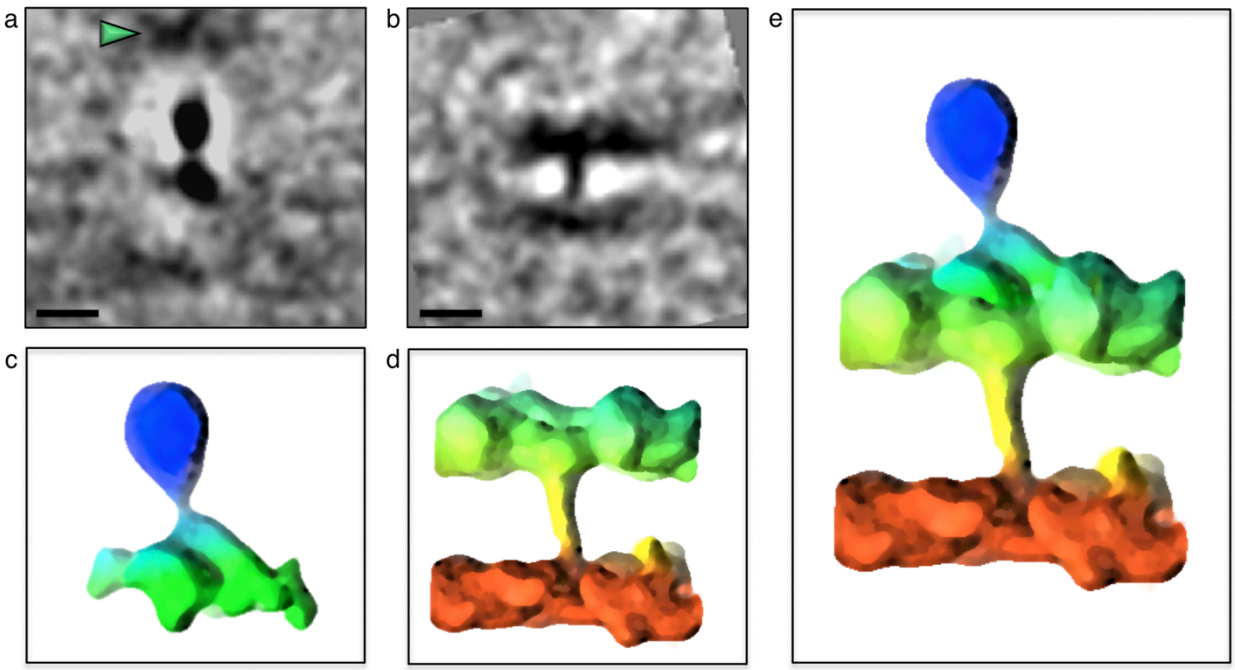

Supplementary Figure 9 – Subtomogram average of the QD-marked supercomplex

Slices through subtomogram averages of the (a) protruding outer membrane and (b) IMS density located directly beneath QD_{605}, scale bars = 10 nm. The density for the QD (green arrowhead in (a)) is less pronounced in the average due to its flexibility relative to the import supercomplex. (c & d) show the corresponding 3D volumes and (e) a composite model of both subtomogram averages. The inner mitochondrial membrane is shown in orange, the IMS protein density in yellow, the mitochondrial outer membrane in green and the outer membrane protein density in blue. Averages were calculated from 81 subvolumes extracted from the 6 tomograms taken at higher magnification with the K2 camera.

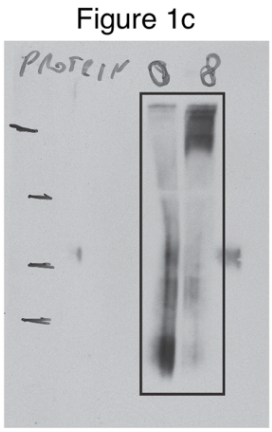

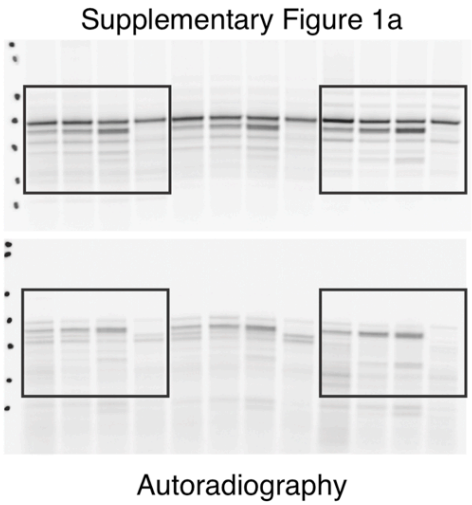

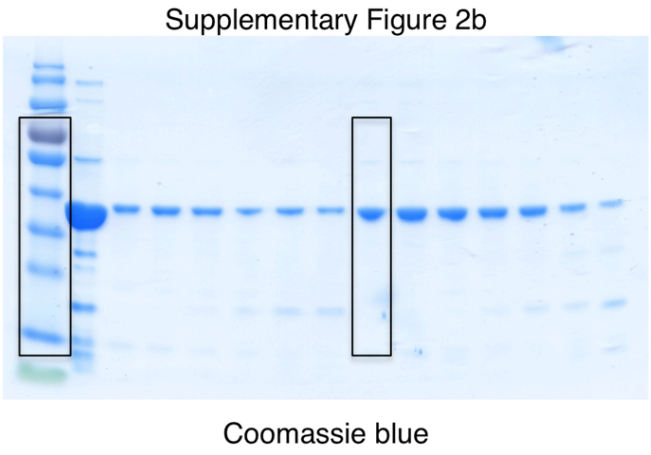

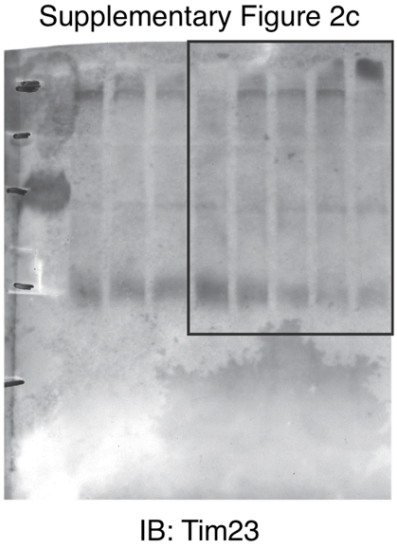

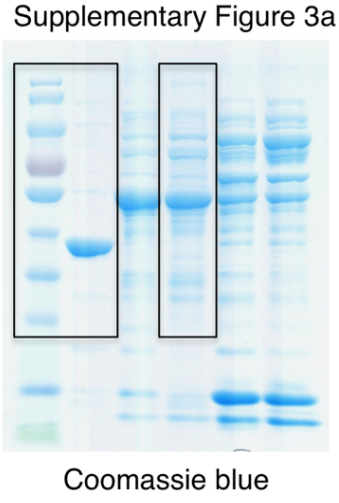

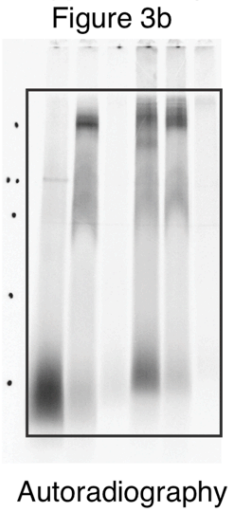

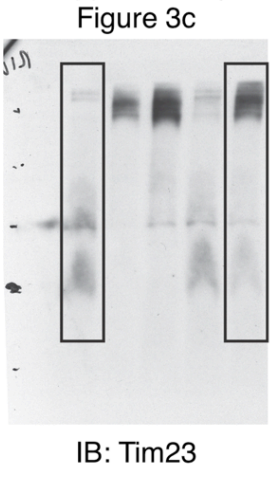

Supplementary Figure 10 – Original scans of the key gels and western blots presented in the paper. IB, immunoblot.

Supplementary Table 1- Primers used in this work

Primer name	Forward (5'-3') primer	Reverse (5'-3') primer	Purpose
C14S	CCTTTACTAAAAATCTCGAAGAACTCTGAGGCTGCTATC	GATAGCAGCCTCAGAGTTCTTCGAGATTTTTAGTAAAGG	Insert mutation C14S into $b_2\Delta$-DHFR
C86S	GCATAACAAGCCCGATGATTCTTGGGTTGTGATCAA	TTGATCACAACCCAAGAATCATCGGGCTTGTTATGC	Insert mutation C86S into $b_2\Delta$-DHFR
C157S	TTCGACCATTGAACTCCATCGTCGCCGTGTC	GACACGGCGACGATGGAGTTCAATGGTCGAA	Insert mutation C157S into $b_2\Delta$-DHFR
D337C	TAAGTTTGAAGTCTACGAGAAGAAATGCTAACAGGAAGATGCTTTCAAGTTC	GAACTTGAAAGCATCTTCCTGTTAGCATTTCTTCTCGTAGACTTCAAACTTA	Insert mutation D337C into $b_2\Delta$-DHFR
$b_2\Delta$-DHFR	GAATACACGGAATTCCCAAACAAAAGTAG	GTTGGGGTCCATGTCTTTCTTCTCGTAG	Amplify $b_2\Delta$-DHFR
MT2/MT3	GAAGAAAGACATGGACCCCAACTGC	GGGTAACGCCAGGGTTTTCC	Amplify MT2 or MT3
pUHE-$b_2\Delta$-DHFR$_{cys}$	GTAGTCCATGGTAAAATACAAACCTTTAC	GACCCAAGCTTGGCCGGATCTAAAGCC	Subclone $b_2\Delta$-DHFR$_{cys}$ from pGEM4 to pUHE-73 vector
pUHE-$b_2\Delta$-DHFR-MT2	GTAGTCCATGGTAAAATACAAACCTTTAC	TTAATACGACTCACTATAGGG	Subclone $b_2\Delta$-DHFR-MT2 from pGEM4 to pUHE-73 vector
pUHE-$b_2\Delta$-DHFR-MT3	GTAGTCCATGGTAAAATACAAACCTTTAC	GGAGACAAGCTTGTCGACTCTAGAGG	Subclone $b_2\Delta$-DHFR-MT3 from pGEM4 to pUHE-73 vector

Supplementary Note 1 – Discussion of the choice of QD and linker

In order to localize the labelled active preprotein import machineries by cryo-ET, we used QD nanoparticles rendered biocompatible by streptavidin-PEG conjugates. There is a variety of options with respect to the size and shape of QDs and linker lengths, which can be chosen to match specific requirements (Supplementary Fig. 4b-d). Single-particle cryo-EM has shown that the TOM complex is an oligomer[5]. Therefore our labelling strategy took into consideration its known dimensions to label as far as possible all mitochondrial translocases present (Fig. 1a). Streptavidin-conjugated QDs bind on average 5-10 streptavidin molecules (Invitrogen, Carlsbad, USA). Consequently, the chance of one QD labelling more than one import site was low when QDs were added in large excess. It is important that proteins or features of interest in the tomographic reconstructions are not obscured by the tag. Therefore, to ensure a sufficient 10 nm distance from QD to membrane, the first experiments were carried out with the smallest commercially available QD (QD_{525}; 4 nm spherical core) with a PEG linker.

Supplementary References

1. Vögtle, F.N., *et al*. Global analysis of the mitochondrial N-proteome identifies a processing peptidase critical for protein stability. *Cell* **139,** 428-439 (2009).
2. Reichert, A.S. & Neupert, W. Contact sites between the outer and inner membrane of mitochondria-role in protein transport. *Biochim Biophys. Acta* **1592,** 41-49 (2002).
3. Dekker, P.J., *et al*. The Tim core complex defines the number of mitochondrial translocation contact sites and can hold arrested preproteins in the absence of matrix Hsp70-Tim44. *EMBO J*. **16,** 5408-5419 (1997).
4. Gebert, M, *et al*. Mgr2 promotes coupling of the mitochondrial presequence translocase to partner complexes. *J. Cell Biol*. **197,** 595-604 (2012).
5. Model, K., Meisinger, C. & Kühlbrandt, W. Cryo-electron microscopy structure of a yeast mitochondrial preprotein translocase. *J. Mol Biol*. **383,** 1049-1057 (2008).